Cell Reports
Report

Fungicidal Drugs Induce a Common Oxidative-Damage Cellular Death Pathway

Peter Belenky,[1,2,3] Diogo Camacho,[1,2,3] and James J. Collins[1,2,3,4,5,*]
[1]Howard Hughes Medical Institute
[2]Department of Biomedical Engineering
[3]Center for BioDynamics
Boston University, Boston, MA 02215, USA
[4]Boston University School of Medicine, Boston, MA 02118, USA
[5]Wyss Institute for Biologically Inspired Engineering, Harvard University, Boston, MA 02115, USA
*Correspondence: jcollins@bu.edu
http://dx.doi.org/10.1016/j.celrep.2012.12.021

SUMMARY

Amphotericin, miconazole, and ciclopirox are antifungal agents from three different drug classes that can effectively kill planktonic yeast, yet their complete fungicidal mechanisms are not fully understood. Here, we employ a systems biology approach to identify a common oxidative-damage cellular death pathway triggered by these representative fungicides in *Candida albicans* and *Saccharomyces cerevisiae*. This mechanism utilizes a signaling cascade involving the GTPases Ras1 and Ras2 and protein kinase A, and it culminates in death through the production of toxic reactive oxygen species in a tricarboxylic-acid-cycle- and respiratory-chain-dependent manner. We also show that the metabolome of *C. albicans* is altered by antifungal drug treatment, exhibiting a shift from fermentation to respiration, a jump in the AMP/ATP ratio, and elevated production of sugars; this coincides with elevated mitochondrial activity. Lastly, we demonstrate that DNA damage plays a critical role in antifungal-induced cellular death and that blocking DNA-repair mechanisms potentiates fungicidal activity.

INTRODUCTION

A rapid rise in immunocompromised patients over the past five decades has led to increasing incidence of systemic fungal infections. Despite current treatment options, the morbidity and mortality rates associated with fungal infections, particularly those of *Candida* species, remain high (Ostrosky-Zeichner et al., 2010).

The polyene amphotericin B (AMB), introduced in the late 1950s, was the first widely used antifungal (AF) drug (Ostrosky-Zeichner et al., 2010). Due to its strong hydrophobicity, AMB penetrates the fungal membrane and binds to ergosterol, leading to membrane damage. Azoles, a second class of AFs, became available in the 1980s and act by inhibiting ergosterol biosynthesis to induce the accumulation of a toxic methylated sterol that stops cell growth (Ostrosky-Zeichner et al., 2010). Although azoles tend to be fungistatic, some azoles such as miconazole (MCZ) can be fungicidal under certain conditions and formulations (Thevissen et al., 2007). Unlike AMB and MCZ, the primary targets of the synthetic AF ciclopirox olamine (CIC) are not fully understood, though some evidence indicates that CIC acts by affecting DNA repair or directly inducing DNA damage (Leem et al., 2003).

Recent work with select AFs has indicated that AF-induced cellular death may follow apoptotic or necrotic pathways that involve the production of reactive oxygen species (ROS) (Phillips et al., 2003; Thevissen et al., 2007) and the modulation of central metabolism (González-Párraga et al., 2011; Yan et al., 2007). However, a comprehensive genetic and metabolic mechanism of AF-induced cellular death remains elusive.

Recent systems biology work from our lab, focused on bacterial cell death, identified a common mechanism of antibiotic action that involves a genetic and metabolic cascade that ultimately results in the formation of toxic ROS (Dwyer et al., 2007; Kohanski et al., 2007, 2008). Aspects of this mechanism have been harnessed to potentiate currently available antibiotics and combat the development of resistance (Dwyer et al., 2009; Kohanski et al., 2007, 2010; Lu and Collins, 2009). Similar approaches to AF mechanisms could provide important, meaningful insights and identify possible means to improve current treatments.

In this work, we apply a systems biology approach to identify mechanisms by which the aforementioned AFs—AMB, MCZ, and CIC—lead to fungal cellular death. We find that, despite their different primary modes of action, all three classes of fungicidal drugs induce a common oxidative-damage cellular death pathway in *Saccharomyces cerevisiae* and *Candida albicans* that involves alterations to cellular metabolism and respiration, culminating in the formation of lethal ROS.

RESULTS

Fungicide-Dependent ROS Production Leads to Fungal Cell Death

Based on previous work that supports the cidal role of ROS production in many modes of fungal death (Breitenbach et al., 2005; Henriquez et al., 2008), we hypothesized that ROS production is critical to AF-induced cellular death. We measured the formation of ROS following AF treatment in yeast using the dye

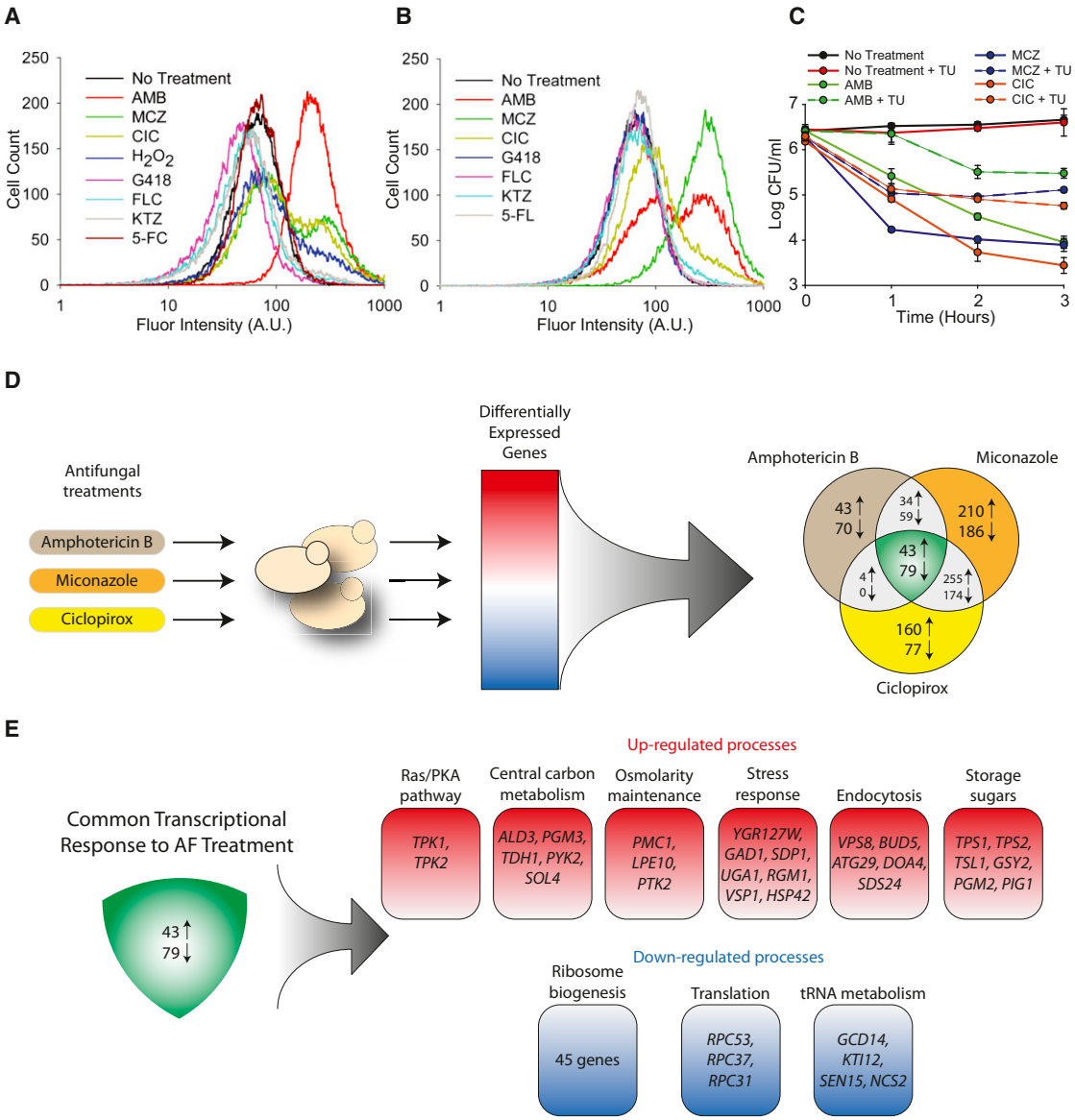

Figure 1. Fungicide-Dependent ROS Production Leads to Fungal Cell Death and a Common Transcriptional Response

(A and B) Generation of ROS as measured by a change in HPF fluorescence after 1.5 hr of drug treatment in *S. cerevisiae* (A) and *C. albicans* (B).

(C) Log of CFU/ml remaining after drug exposure in the presence and absence of 50 mM thiourea (TU). Drug concentrations used: AMB 1 μg/ml, MCZ 50 μg/ml, CIC 75 μg/ml, H_2O_2 1 mM, geneticin (G418) 100 μg/ml, fluconazole (FLC) 50 μg/ml, 5-flucytosine (5-FC) 15 μg/ml, and ketoconazole (KTZ) 50 μg/ml. The reported error is SD with n ≥ 3.

(D) A common transcriptional response to AF treatment was identified by performing differential expression analysis against a compendium of expression arrays. The common set of differentially expressed genes is represented by the intersection of the three sets of genes.

(E) Pathway analysis of the common set of differentially expressed genes identified six major processes that are upregulated in response to AFs and three processes that are downregulated under the same treatments.

See also Figure S1 and Table S1.

3′-(p-hydroxyphenyl) fluorescein (HPF), which is preferentially oxidized by intracellular hydroxyl radicals into a fluorescent product (Kohanski et al., 2007). We treated exponentially growing wild-type *S. cerevisiae* and *C. albicans* in synthetic dextrose complete (SDC) medium with the minimum concentration of fungicide required to achieve at least a 90% reduction in colony-forming units (CFU) after 3 hr of exposure. As a positive control, we also treated cells with H_2O_2, a potent inducer of hydroxyl radical formation (Perrone et al., 2008). After 1.5 hr of treatment, we found that all tested fungicidal drugs and H_2O_2 lead to dramatic induction of HPF fluorescence (Figure 1A, 1B, and S1), indicating that all tested fungicidal agents induce the formation of ROS. Conversely, fungistatic drugs added at concentrations 10-fold above the minimal inhibitory concentration

or at the maximum soluble concentration did not lead to detectable ROS formation (Figures 1A, 1B, and S1).

To test whether the observed production of ROS contributes to AF-induced cellular death, we treated cells with thiourea, a potent scavenger of hydroxyl radicals in eukaryotic and prokaryotic cells (Kohanski et al., 2007; Touati et al., 1995). We found that exposing exponentially growing *S. cerevisiae* to 50 mM thiourea for 30 min prior to the addition of AF drugs considerably diminished the toxicity of all three AFs, reducing killing at 3 hr by ~15-fold for AMB and CIC and by ~10-fold for MCZ (Figure 1C). These results indicate that ROS production plays a critical role in cellular death following treatment by AMB, MCZ, and CIC.

Identifying a Common Transcriptional Response to AF Treatment

To build a comprehensive model of the yeast response to AFs, we measured changes in global gene expression of *S. cerevisiae* following treatment with AMB, MCZ, and CIC. To assess the effect of each AF treatment on gene expression, we performed a z-test between experiment and control samples, where the average and SD for the expression of each gene was calculated across a compendium of publically available expression data sets (see Extended Experimental Procedures). We compared the differential gene-expression profile of each treatment at each time point to the no-treatment control to identify the set of genes commonly perturbed by fungicide treatment (Figure 1D). This analysis revealed that 43 genes were commonly upregulated under AF treatment, while 79 genes were downregulated under the same conditions (Figure 1E). To investigate the biological pathways and processes in which these genes are involved, we ran a functional enrichment analysis on Gene Ontology (GO) terms associated with each one of these genes. The analysis was conducted with the *Saccharomyces* Genome Database's GO Term Finder tool using default parameters. The majority of the commonly downregulated genes are involved in protein synthesis, specifically, ribosomal biogenesis and tRNA synthesis. The 43 commonly upregulated genes fall into six general biological processes: the production of storage sugars, endocytosis, general stress response, osmolarity maintenance, central carbon metabolism, and the RAS/protein kinase A (PKA) signaling pathway (Figure 1E).

Our expression analysis identified the production of storage sugars as a key process upregulated following AF treatment. Specifically, genes involved in glycogen metabolism and the production of the storage sugar trehalose were robustly upregulated after the addition of fungicides (Figure 1E; Table S1). Cellular production of trehalose and glycogen are energy-expensive pathways that consume significant amounts of ATP. Consistent with this, the activation of the trehalose pathway has been shown to increase ATP consumption, mitochondrial enzyme content, and respiration (Noubhani et al., 2009). Thus, the production of these sugars may contribute to increased mitochondrial activity and elevated ROS production.

TCA Cycle and Electron Transport Chain Play Critical Roles in AF-Induced Cell Death

To identify genes critical to AF action, we tested the AF sensitivity of single-gene knockouts identified through our common transcriptional analysis. In total, we tested the AF sensitivities of 81 single-gene knockouts (Table S2) and found that 12 of them had increased resistance to all three AFs (AMB, MCZ, CIC).

Actively respiring, energy-producing mitochondria are the major source of ROS in yeast cells. However, *S. cerevisiae* respiratory activity is usually repressed under normal growth conditions in the presence of glucose (Hardie et al., 1999), though various stress responses have been shown to upregulate respiratory genes even in the presence of glucose (Gasch et al., 2000). We therefore hypothesized that treatment with fungicides induces a switch from normal fermentative growth to mitochondrial respiration.

To assess the role of mitochondrial respiration in AF-induced cellular death, we first analyzed the expression of mitochondrial genes in *S. cerevisiae* in response to AF treatment (Table S1). Of particular interest, we found that the gene encoding the rate-limiting step of the tricarboxylic acid (TCA) cycle, citrate synthase-1 (*CIT1*), exhibited a slight increase in expression across all AF treatments. The induction of *CIT1* is a hallmark of stress-induced respiration (Gasch et al., 2000). We found that deleting *CIT1*, *CIT2*, or *CIT3* dramatically reduced yeast sensitivity to all three AFs when compared to the wild-type *S. cerevisiae* strain (Figures 2A and S2). To parse out the role of the various citrate syntheses in AF-induced cellular death, we created single and double deletions of *CIT1* and *CIT2* in the *cit3* background. We found that deleting the remaining citrate synthases in this background provides additive resistance to AMB, with the triple mutant requiring more than 8-fold-higher drug concentrations to achieve the sensitivity of the single mutants (Figures 2C). Interestingly, a similar additive effect was not observed with MCZ or CIC, indicating that AMB toxicity is more sensitive to further changes in citrate metabolism than the other two drugs.

We also found that deleting succinate dehydrogenases (*SDH1* or *SDH2*), enzymes that couple the oxidation of succinate to the transfer of electrons to the mitochondrial electron transport chain (ETC) (Chapman et al., 1992), decreased drug susceptibility. Additionally, we found that disrupting the TCA cycle at these two key points reduces the AF-dependent production of ROS (Figure 2B), indicating that this phenomenon involves the TCA cycle.

The TCA cycle produces NADH, which is then fed into the ETC to produce ATP. This activity also leads to the production of ROS as a byproduct of aerobic respiration. We therefore targeted the first committed steps of the ETC by deleting the intramitochondrial NADH dehydrogenase (*NDI1*) and the external NADH dehydrogenase (*NDE1*). The *NDI1* and *NDE1* deletions exhibited increased resistance to all three AF drugs and a concomitant reduction in AF-dependent ROS production (Figures 2A and 2B).

We next sought to assess the mitochondrial activity of AF-treated fungal cells. We utilized the MitoTracker Red dye, which enters the mitochondrial matrix by utilizing the proton motive force and thus labels metabolically active mitochondria in viable cells (Arita et al., 2006; Tomas et al., 2011). We incubated exponential phase *S. cerevisiae* in glucose-free synthetic complete (SC) media for 30 min and then switched them to SC containing 2% glucose or nonfermentable acetate for 1.5 hr. As expected, we detected approximately 5-fold more MitoTracker fluorescence in acetate-incubated cells (Figure 2D), indicating that the dye specifically labels cells with activated mitochondria. Adding

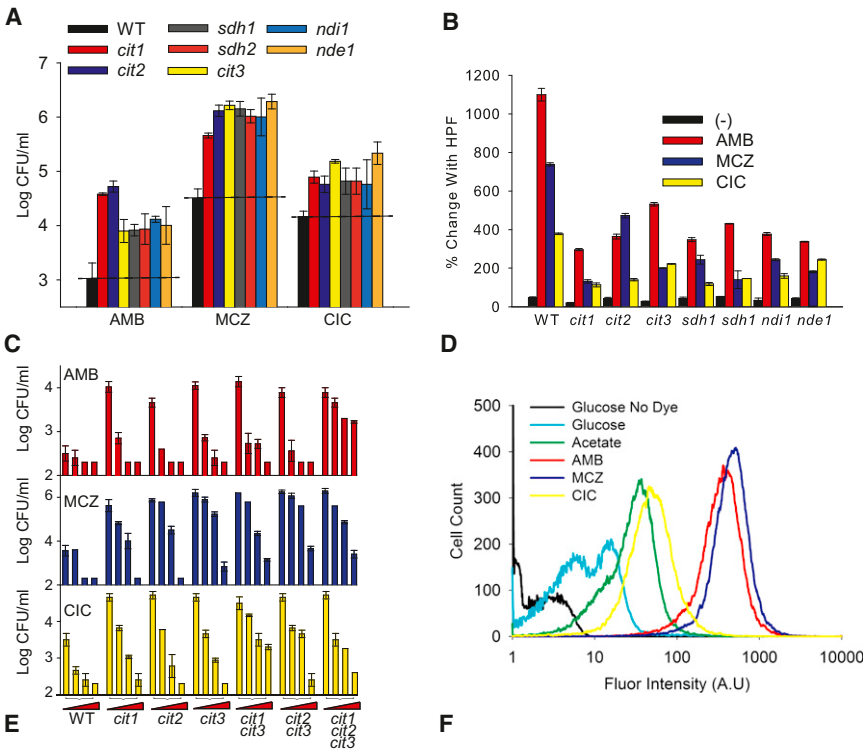

Figure 2. TCA-Dependent Respiration and the Ras/PKA Pathway Play a Critical Role in AF-Induced Cell Death

(A and E) Log of CFU/ml remaining after 3 hr of drug exposure of wild-type *S. cerevisiae* and mutants targeting the TCA cycle, respiration, and the Ras/PKA pathway.

(B and F) Cellular ROS levels quantified as percent change in fluorescence after the addition of HPF. The indicated strains were treated with AF drugs for 1 hr prior to the addition of HPF. Drug concentrations used: AMB 1 μg/ml, MCZ 50 μg/ml, and CIC 75 μg/ml.

(C) Log of CFU/ml remaining after 3 hr of drug exposure. Drug concentrations used, increasing from left to right: AMB (1 μg/ml, 1.5 μg/ml, 2.5 μg/ml, and 8 μg/ml), MCZ (50 μg/ml, 75 μg/ml, 100 μg/ml, and 150 μg/ml), and CIC (75 μg/ml, 100 μg/ml, 125 μg/ml, and 150 μg/ml). The reported error is SD with $n \geq 3$.

(D) Yeast mitochondrial content assayed by fluorescent staining with MitoTracker Red probe after 1 hr of exposure to the indicated drug or metabolite.

See also Figure S2 and Table S2.

CIC, AMB, or MCZ to glucose-incubated cells increased MitoTracker fluorescence by 10-fold, 60-fold, and 70-fold, respectively (Figure 2D). All three drugs induced considerably more mitochondrial activity than acetate, indicating that AF treatment has a greater impact on mitochondrial activity than normal respiratory metabolism. These results are consistent with our hypothesis that AF drugs induce a shift from fermentative growth to ROS-producing mitochondrial respiration.

RAS/PKA Pathway Is a Key Mediator of AF Toxicity

Having established that AFs induce mitochondrial-dependent ROS production, we next sought to ascertain the signaling events that lead to these metabolic changes. The RAS/PKA pathway, consisting of two GTPases (Ras1 and 2) and three PKA isoforms (Tpk1-3), has been shown to respond to cellular stress by inducing mitochondrial biogenesis and cellular death through the production of ROS via disordered mitochondrial respiration (Chevtzoff et al., 2010; Leadsham and Gourlay, 2010; Thevelein and de Winde, 1999). We found that aspects of this signaling pathway were upregulated in response to AFs (Table S1). For example, *TPK1* and *TPK2* were robustly induced in response to AF treatment, and we found an increase in expression of other genes involved in the same pathway (Table S1), namely, *BMH2*, *CYR1*, and *SRV2*. Further, we found that *PDE2*, the cyclic AMP phosphodiesterase that represses the RAS/PKA signaling, was significantly downregulated. Deleting *PDE2* in the presence of activated RAS/PKA signaling has been shown to lead to the overproduction of ROS by dysfunctional mitochondria, resulting in cellular death (Leadsham and Gourlay, 2010). Together, these results indicate that the RAS/PKA signaling pathway is largely upregulated in response to AF treatment and may contribute to the production of ROS by mitochondria.

We tested the role of the RAS/PKA pathway in AF-induced cellular death by studying single-gene knockouts of the upstream and downstream portions of the pathway. We found that deleting either *RAS1* or *RAS2* reduced yeast susceptibility to all three AFs (Figures 2E and S2) and deleting the downstream effector kinases, *TPK1, TPK2* and *TPK3*, also reduced or delayed killing. Additionally we found that deleting any one of the key members of the RAS/PKA signaling pathway reduced the drug-dependent buildup of ROS (Figure 2F). This finding suggests that RAS/PKA signaling is critical for the induction of mitochondrial ROS production in response to drug treatment.

Common Metabolic Changes Resulting from AF Treatment

Our results link AF treatment to distinct changes in intracellular metabolic activity as part of an induced common killing

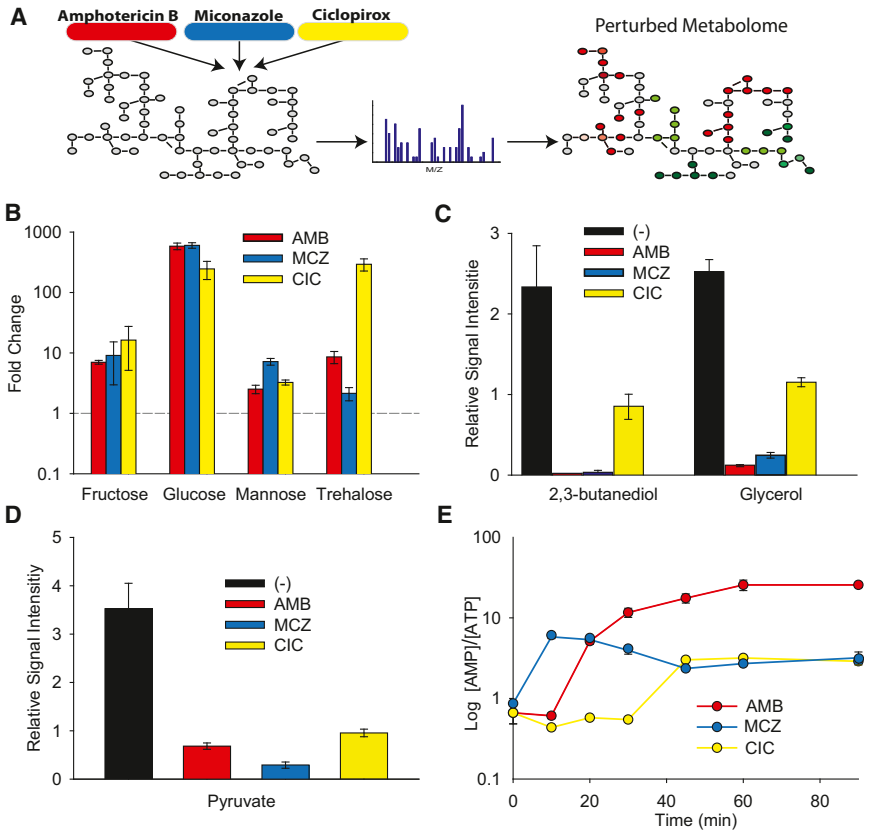

Figure 3. AF Treatment Leads to Common Metabolic Changes Resulting in the Production of Sugars and a Dramatic Reduction of ATP Levels

(A) A schematic of the metabolomics study. Cells were treated with AF drugs for 1.5 hr and intracellular metabolites were analyzed using mass spectrometry to identify the AF-perturbed metabolome.

(B) Fold change in metabolite levels compared to the no-treatment control.

(C and D) Relative signal intensity of select metabolites identified through metabolomic profiling of *C. albicans* exposed to AF drugs for 1.5 hr. Drug concentrations used: AMB 1 μg/ml, MCZ 50 μg/ml, and CIC 75 μg/ml. The reported error is SEM with n = 6.

(E) AMP/ATP ratio in *C. albicans* treated with drugs over a 90 min period. Drug concentrations used: AMB 0.35 μg/ml, MCZ 50 μg/ml, and CIC 75 μg/ml. The reported error is SD with an $n \geq 3$.

See also Figures S3 and S4.

mechanism. To further explore the role of metabolism in AF-induced cellular death, we directly measured the effect of AF treatment on the intracellular metabolome of *C. albicans*. To do so, we utilized a platform for metabolite detection and relative quantification from Metabolon (Durham, NC, USA) (Evans et al., 2009). We treated exponentially growing *C. albicans* cells with AFs and collected samples for metabolomic analysis after 1.5 hr of treatment, a time point when we expected at least 90% of cells contributing to the metabolite pool to be irreversibly committed to the death pathway (Figure S3). We found that the three drug treatments (AMB, MCZ, and CIC) significantly changed ($p \leq 0.05$) the relative abundance of between 155 and 213 metabolites when compared to the no-treatment controls (Data Set S1).

Glucose was the most highly induced metabolite, found to be greater than 600-fold more abundant in drug-treated cells (Figure 3B). Other carbohydrates, such as fructose and mannose, were also significantly more abundant in all of the treatment groups compared to the control, as was the disaccharide trehalose (Figure 3B). These results are consistent with our microarray data that identified the upregulation of polysaccharide biosynthesis as an important transcriptional response to AF treatment.

Our phenotypic analyses in *S. cerevisiae* suggested that cells may be switching from exclusively fermentative growth to mitochondrial respiration in response to AF treatment. Consistent with this result, we found that 2,3-butanediol and glycerol, two major fermentative waste products (González et al., 2000), were substantially reduced after AF treatment (Figure 3C). Furthermore, pyruvate levels were dramatically lower in drug-treated samples (Figure 3D), indicating possible consumption by the TCA cycle; of note, TCA cycle intermediates were also reduced (Data Set S1) in comparison to the untreated cells. These measurements, combined with our genetic data and measurements of mitochondrial activity and biogenesis, provide support for a common fungicidal mechanism of action that relies on reduced fermentation and induced ROS-producing mitochondrial respiration.

The dramatic elevation of intracellular sugars and the shift from fermentation to respiration suggests that the AF treatments may be increasing ATP consumption. Abundant nucleotides such as ATP are not accurately quantified using the metabolic platform we selected for this study. We therefore sought to measure ATP levels over time using high-performance liquid chromatography (HPLC). We analyzed the AMP/ATP levels in lysates collected from cells treated with the three AFs. We found that the AF treatments elevated the AMP/ATP ratio by between 4- and 24-fold (Figure 3E), through a large drop in ATP levels and a proportional rise in AMP levels. ATP levels are normally static but can change dramatically under severe stress conditions that induce necrosis (Henriquez et al., 2008; Osório et al., 2004). Our results suggest that fungicide-stimulated sugar production induces a necrosis-like rapid consumption of ATP.

DNA Repair Is a Critical Response to AF-Dependent ROS Production

ROS damage multiple cellular targets, including membranes, proteins, and DNA (Kohanski et al., 2007; Salmon et al., 2004). Recent work indicates that DNA repair, specifically double-strand break repair (DSBR), plays a critical role in *C. albicans* resistance to oxidative damage (Legrand et al., 2007, 2008).

We chose to analyze the role of DNA repair in AF-induced cellular death by testing the susceptibility of *C. albicans* strains with deletions of critical genes in nucleotide excision repair, mismatch repair, and DSBR. We used AMB, MCZ, and CIC at a range of concentrations and found that DSBR mutants were particularly susceptible to all three AFs when compared to wild-type (Figures 4A–4C). Specifically, we found that the minimal fungicidal concentrations for the DSBR mutants, *rad50*/*rad50* and *rad52*/*rad52*, were reduced by as much as 10-fold compared to wild-type.

Next we utilized the TUNEL assay to quantify the relative abundance of double-strand breaks in *C. albicans* cells treated with AFs and H_2O_2. The TUNEL reagent fluorescently labels both double- and single-strand DNA breaks (Ribeiro et al., 2006). Treating cells with AFs and H_2O_2 elevated relative fluorescence as measured by flow cytometry (Figure 4D), indicating a considerable induction of DNA breaks.

We also assayed *rad50* and *rad52* knockouts in *S. cerevisiae* to test whether the role of DNA damage in AF toxicity is consistent with the results from *C. albicans*. We found that these mutants were considerably more susceptible to H_2O_2 and AFs than wild-type *S. cerevisiae*, although the differences were smaller than those seen with *C. albicans.* Together, these data provide support for the role of DNA damage as a factor contributing to a common mechanism of AF action and indicate that targeting DNA-repair mechanisms could be an effective means for potentiating fungicidal activity.

For additional details, please see Extended Results.

DISCUSSION

In this work, we utilized a systems biology approach to study the response of fungal cells to AF treatment. We found that despite divergent primary modes of action, fungicides from three distinct classes induce a common signaling and metabolic cascade that leads to ROS-dependent cellular death (Figure 4I). We propose that cellular changes and damage initiated through interaction with primary targets of AFs result in activation of a stress-like response that includes signaling through the RAS/PKA pathway. Through this and possibly other pathways, cells activate mitochondrial activity and shift from fermentation to respiration in response to AFs. This abrupt induction of mitochondrial activity leads to the overproduction of toxic ROS in a manner that depends on the TCA cycle and ETC. Additionally, we found that AF treatment leads to a buildup of monosaccharides and disaccharides, including glucose and trehalose. Both the import and synthesis of these sugars are energetically expensive, requiring the consumption of ATP and the production of AMP. It is likely that these metabolic changes lead to altered respiration and the overproduction of ROS by dysfunctional mitochondria, ultimately resulting in cell death (Figure 4I).

The common AF-dependent responses identified in this work have similarities to many fungal stress-response mechanisms (Gasch et al., 2000; Soufi et al., 2009), suggesting that AF agents may function by overactivating these pathways to induce cellular death. These similarities include a collapse of ATP levels (Osório et al., 2004), mitochondrial dysfunction that leads to the production of ROS (Breitenbach et al., 2005), and a central role played by the RAS/PKA pathway (Estruch, 2000). It is likely that AFs cause cellular damage that mirrors the effects of osmotic, heat, and alcohol stress, leading to the induction of stress-related pathways. Interestingly, the same responses that protect cells from mild environmental stress may in fact contribute to AF-dependent cellular death. AF insult to fungal cells may be sufficiently powerful such that the overactivation of these general stress responses does not protect the cell, but instead plays a net contributory role in cellular death through the consumption of ATP and the production of ROS.

In addition to similarities with known fungal stress pathways, the identified common mechanism of AF-induced fungal cellular death can also be compared to the previously identified common mechanism of antibiotic-mediated bacterial cellular death (Dwyer et al., 2007; Kohanski et al., 2007). Despite the complex and multilayered eukaryotic mechanism, robust similarities can be found between the two phenomena, indicating possible evolutionary conservation. In both prokaryotes and eukaryotes, cellular damage resulting from the primary drug-target interaction activates key metabolic regulators, such as RAS in yeast and ArcA in bacteria (Kohanski et al., 2008). These universal regulators modulate central metabolism through the induction of the TCA cycle and respiratory activity to produce toxic ROS.

The endpoint of the common antimicrobial mechanisms in both bacteria and yeast is cellular death through the production of toxic ROS. In both prokaryotes and eukaryotes, ROS induces double-strand DNA breaks (Dwyer et al., 2012; Foti et al., 2012) and other forms of cellular damage that lead to cellular death and are potentiated by blocking DNA repair. In yeast, we demonstrated that by blocking DSBR we could reduce the minimal fungicidal concentration of the tested AF drugs by as much as 10-fold. Similarly, deleting RecA, an *Escherichia coli* homolog of the yeast *RAD* genes, substantially enhances bactericidal antibiotic activity in bacteria (Kohanski et al., 2007). These findings suggest that inhibitors of DNA repair mechanisms may be robust potentiators of fungicides and bactericidal antibiotics.

The critical role of ROS in antimicrobial activity indicates that ROS generation may have evolved and been maintained in both prokaryotes and eukaryotes as a central mechanism to overcome environmental stress. Under various stress conditions, low-level ROS production can activate multiple protective responses including the upregulation of antioxidant enzymes and the induction of beneficial mutations (Belenky and Collins, 2011; Gems and Partridge, 2008; Kohanski et al., 2010). However, if ROS production goes above a certain threshold, it no longer serves a protective role and instead induces cellular death. Thus, it is likely that many lethal challenges, including fungicides, function by highjacking natural stress-response mechanisms to induce ROS production above this threshold.

EXPERIMENTAL PROCEDURES

Fungal Strains and Media

S. cerevisiae strains used in this work were derivatives of BY4742, created as part of the Deletion Consortium (Winzeler et al., 1999). Deletion Consortium

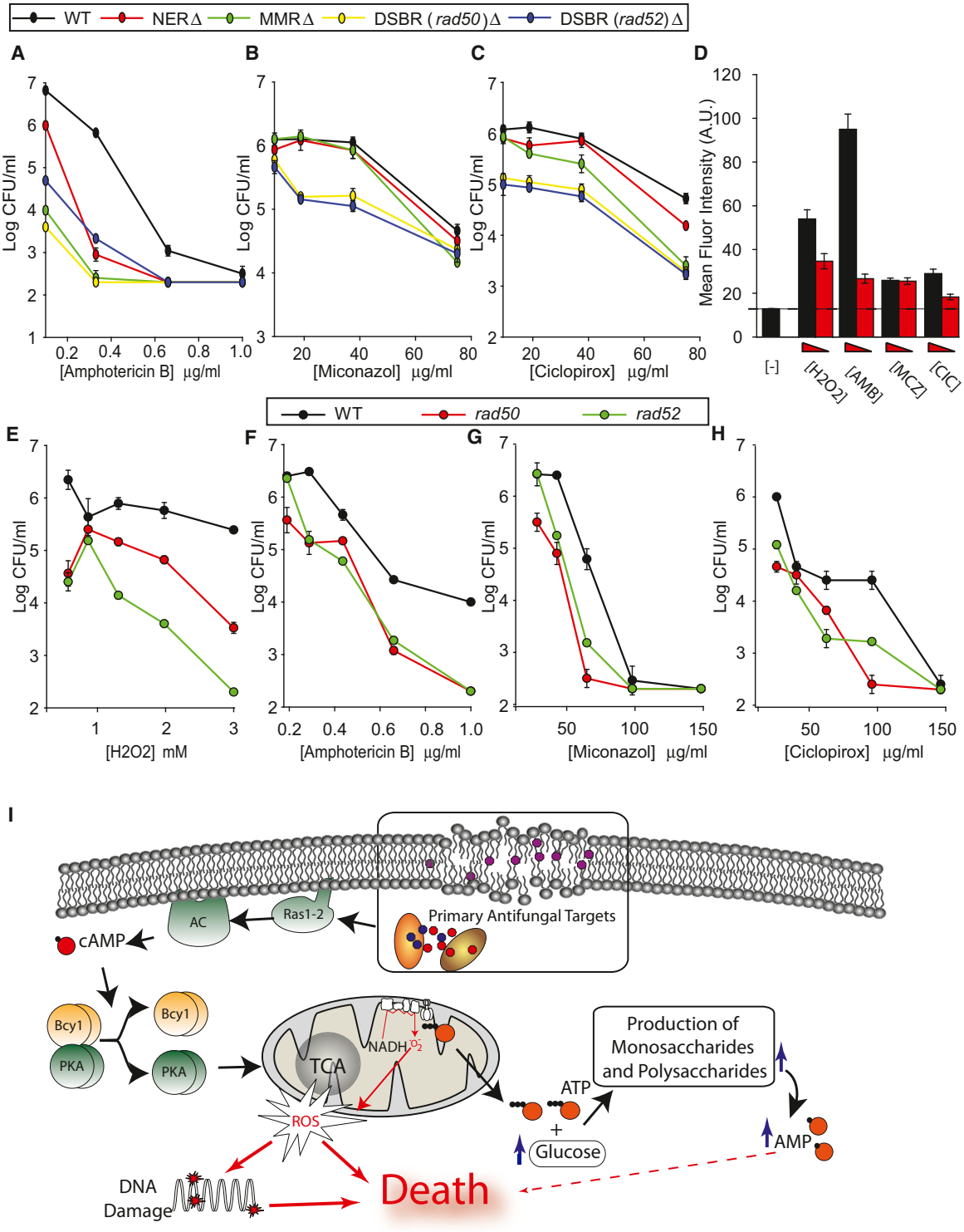

Figure 4. DNA Repair Is a Critical Response to AF-Dependent ROS Production

(A–C) Log of CFU/ml remaining after 3 hr of drug exposure of wild-type *C. albicans* and mutants targeting DSBR (*rad50*/*rad50* and *rad52*/*rad52*), nucleotide excision (NER [*rad10*/*rad10*]), and mismatch (MMR [*msh1*/*msh1*]) DNA-repair mechanisms.

(D) TUNEL staining of exponentially growing cells assayed by flow cytometry after 2 hr of treatment. Drug concentrations used, decreasing from left to right: H_2O_2 (10 mM and 5 mM), AMB (1 µg/ml and 0.5 µg/ml), MCZ (100 µg/ml and 50 µg/ml), and CIC (150 µg/ml and 75 µg/ml).

(E–H) Log of CFU/ml remaining after 3 hr of drug exposure of wild-type *S. cerevisiae* and mutants targeting DSBR. The reported error is SD with $n \geq 3$.

(legend continued on next page)

strains with reported phenotypes were verified by PCR. Stains PAB202 (BY4742 cit1Δ::kanMX4 cit3Δ::URA3), PAB205 (BY4742 cit3Δ::kanMX4 cit2Δ::LEU2), and PAB208 (PAB202 cit2Δ::LEU2) were created by direct transformation of PCR products as previously described (Brachmann et al., 1998). *S. cerevisiae rad50* and *rad52* knockouts were derivatives of MKP-0 and generously provided to us by Dr. Simone Moertl (Steininger et al., 2010). Wild-type *C. albicans* strain, SC5314, was used in metabolomic profiling and HPF measurements. *C. albicans* DNA repair mutants used in this work were derivatives of DKCa39, generously provided by Dr. David T. Kirkpatrick. A complete list of DKCa strains used in this study is provided in Table S3. SDC media and synthetic complete media with 2% acetate (pH 6.5) were prepared as previously described (Burke et al., 2000; Wickerham, 1946).

Fungicidal Killing and Fluorescent Dye Assays

Overnight yeast cultures were diluted into the indicated media and grown to an optical density 600 of 0.2, at which point the AFs were added. CFU were measured by plating six serial dilutions onto YPD agar plates. A more detailed description is included in Extended Experimental Procedures.

S. cerevisiae Microarrays

Yeast cells were incubated in 25 ml SDC and grown in 250 ml flasks at 30°C and 300 rpm. AFs were added at an OD600 of 0.2. Cells were harvested after treatment and their RNA was isolated and processed as previously described (Schmitt et al., 1990). The complete microarray analysis procedures are described in Extended Experimental Procedures.

Metabolomic Profiling

C. albicans cells were lysed and assayed by Metabolon as previously described (Shakoury-Elizeh et al., 2010). ATP and AMP were extracted as previously described (Walther et al., 2010) and analyzed by HPLC. This procedure is more fully described in Extended Experimental Procedures.

ACCESSION NUMBERS

The compendium containing 536 microarrays has been deposited to the Many Microbe Microarrays Database database (http://m3d.bu.edu/) at http://m3d.bu.edu/datasets/Belenky_scerevisiae_compendium.txt.tar.gz.

SUPPLEMENTAL INFORMATION

Supplemental Information includes Extended Results, Extended Experimental Procedures, four figures, three tables, and a data set and can be found with this article online at http://dx.doi.org/10.1016/j.celrep.2012.12.021.

LICENSING INFORMATION

ACKNOWLEDGMENTS

We thank David T. Kirkpatrick for the set of DKCa strains, Simone Moertl for the MKP-0 strains, Merck & Co. for providing caspofungin, Katie Vignola and Tim Hyde at Metabolon for their help with metabolomic profiling, and Norman Gerry (Coriell Institute) for processing the microarrays. This work was supported by the Howard Hughes Medical Institute and a National Institutes of Health Director's Pioneer Award (DP1 OD003644).

Received: July 12, 2012
Revised: November 28, 2012
Accepted: December 18, 2012
Published: February 14, 2013

REFERENCES

Arita, Y., Harkness, S.H., Kazzaz, J.A., Koo, H.C., Joseph, A., Melendez, J.A., Davis, J.M., Chander, A., and Li, Y. (2006). Mitochondrial localization of catalase provides optimal protection from H2O2-induced cell death in lung epithelial cells. Am. J. Physiol. Lung Cell. Mol. Physiol. *290*, L978–L986.

Belenky, P., and Collins, J.J. (2011). Microbiology. Antioxidant strategies to tolerate antibiotics. Science *334*, 915–916.

Brachmann, C.B., Davies, A., Cost, G.J., Caputo, E., Li, J., Hieter, P., and Boeke, J.D. (1998). Designer deletion strains derived from Saccharomyces cerevisiae S288C: a useful set of strains and plasmids for PCR-mediated gene disruption and other applications. Yeast *14*, 115–132.

Breitenbach, M., Laun, P., and Gimona, M. (2005). The actin cytoskeleton, RAS-cAMP signaling and mitochondrial ROS in yeast apoptosis. Trends Cell Biol. *15*, 637–639.

Burke, D., Dawson, D., and Stearns, T. (2000). Methods in Yeast Genetics (Cold Spring Harbor, NY: Cold Spring Harbor Press).

Chapman, K.B., Solomon, S.D., and Boeke, J.D. (1992). SDH1, the gene encoding the succinate dehydrogenase flavoprotein subunit from Saccharomyces cerevisiae. Gene *118*, 131–136.

Chevtzoff, C., Yoboue, E.D., Galinier, A., Casteilla, L., Daignan-Fornier, B., Rigoulet, M., and Devin, A. (2010). Reactive oxygen species-mediated regulation of mitochondrial biogenesis in the yeast Saccharomyces cerevisiae. J. Biol. Chem. *285*, 1733–1742.

Dwyer, D.J., Kohanski, M.A., Hayete, B., and Collins, J.J. (2007). Gyrase inhibitors induce an oxidative damage cellular death pathway in Escherichia coli. Mol. Syst. Biol. *3*, 91.

Dwyer, D.J., Kohanski, M.A., and Collins, J.J. (2009). Role of reactive oxygen species in antibiotic action and resistance. Curr. Opin. Microbiol. *12*, 482–489.

Dwyer, D.J., Camacho, D.M., Kohanski, M.A., Callura, J.M., and Collins, J.J. (2012). Antibiotic-induced bacterial cell death exhibits physiological and biochemical hallmarks of apoptosis. Mol. Cell *46*, 561–572.

Estruch, F. (2000). Stress-controlled transcription factors, stress-induced genes and stress tolerance in budding yeast. FEMS Microbiol. Rev. *24*, 469–486.

Evans, A.M., DeHaven, C.D., Barrett, T., Mitchell, M., and Milgram, E. (2009). Integrated, nontargeted ultrahigh performance liquid chromatography/electrospray ionization tandem mass spectrometry platform for the identification and relative quantification of the small-molecule complement of biological systems. Anal. Chem. *81*, 6656–6667.

Foti, J.J., Devadoss, B., Winkler, J.A., Collins, J.J., and Walker, G.C. (2012). Oxidation of the guanine nucleotide pool underlies cell death by bactericidal antibiotics. Science *336*, 315–319.

Gasch, A.P., Spellman, P.T., Kao, C.M., Carmel-Harel, O., Eisen, M.B., Storz, G., Botstein, D., and Brown, P.O. (2000). Genomic expression programs in the response of yeast cells to environmental changes. Mol. Biol. Cell *11*, 4241–4257.

Gems, D., and Partridge, L. (2008). Stress-response hormesis and aging: "that which does not kill us makes us stronger". Cell Metab. *7*, 200–203.

González, E., Fernández, M.R., Larroy, C., Solà, L., Pericàs, M.A., Parés, X., and Biosca, J.A. (2000). Characterization of a (2R,3R)-2,3-butanediol

(I) The proposed common mechanism of AF action for the tested fungicides: AF activity against primary intracellular targets leads to cellular changes sensed by the RAS/PKA signaling pathway. The RAS/PKA signaling cascade induces mitochondrial activity, leading to the production of ROS. Simultaneously, the production of sugars, consistent with the fungal stress response, leads to the rapid consumption of ATP and the production of AMP. Elevated intracellular ROS production leads to cellular death through damage to DNA and other cellular targets.
See also Table S3.

dehydrogenase as the Saccharomyces cerevisiae YAL060W gene product. Disruption and induction of the gene. J. Biol. Chem. *275*, 35876–35885.

González-Párraga, P., Sánchez-Fresneda, R., Zaragoza, O., and Argüelles, J.C. (2011). Amphotericin B induces trehalose synthesis and simultaneously activates an antioxidant enzymatic response in Candida albicans. Biochim. Biophys. Acta *1810*, 777–783.

Hardie, D.G., Salt, I.P., Hawley, S.A., and Davies, S.P. (1999). AMP-activated protein kinase: an ultrasensitive system for monitoring cellular energy charge. Biochem. J. *338*, 717–722.

Henriquez, M., Armisén, R., Stutzin, A., and Quest, A.F. (2008). Cell death by necrosis, a regulated way to go. Curr. Mol. Med. *8*, 187–206.

Kohanski, M.A., Dwyer, D.J., Hayete, B., Lawrence, C.A., and Collins, J.J. (2007). A common mechanism of cellular death induced by bactericidal antibiotics. Cell *130*, 797–810.

Kohanski, M.A., Dwyer, D.J., Wierzbowski, J., Cottarel, G., and Collins, J.J. (2008). Mistranslation of membrane proteins and two-component system activation trigger antibiotic-mediated cell death. Cell *135*, 679–690.

Kohanski, M.A., DePristo, M.A., and Collins, J.J. (2010). Sublethal antibiotic treatment leads to multidrug resistance via radical-induced mutagenesis. Mol. Cell *37*, 311–320.

Leadsham, J.E., and Gourlay, C.W. (2010). cAMP/PKA signaling balances respiratory activity with mitochondria dependent apoptosis via transcriptional regulation. BMC Cell Biol. *11*, 92.

Leem, S.H., Park, J.E., Kim, I.S., Chae, J.Y., Sugino, A., and Sunwoo, Y. (2003). The possible mechanism of action of ciclopirox olamine in the yeast Saccharomyces cerevisiae. Mol. Cells *15*, 55–61.

Legrand, M., Chan, C.L., Jauert, P.A., and Kirkpatrick, D.T. (2007). Role of DNA mismatch repair and double-strand break repair in genome stability and antifungal drug resistance in Candida albicans. Eukaryot. Cell *6*, 2194–2205.

Legrand, M., Chan, C.L., Jauert, P.A., and Kirkpatrick, D.T. (2008). Analysis of base excision and nucleotide excision repair in Candida albicans. Microbiology *154*, 2446–2456.

Lu, T.K., and Collins, J.J. (2009). Engineered bacteriophage targeting gene networks as adjuvants for antibiotic therapy. Proc. Natl. Acad. Sci. USA *106*, 4629–4634.

Noubhani, A., Bunoust, O., Bonini, B.M., Thevelein, J.M., Devin, A., and Rigoulet, M. (2009). The trehalose pathway regulates mitochondrial respiratory chain content through hexokinase 2 and cAMP in Saccharomyces cerevisiae. J. Biol. Chem. *284*, 27229–27234.

Osório, H., Moradas-Ferreira, P., Günther Sillero, M.A., and Sillero, A. (2004). In Saccharomyces cerevisiae, the effect of H2O2 on ATP, but not on glyceraldehyde-3-phosphate dehydrogenase, depends on the glucose concentration. Arch. Microbiol. *181*, 231–236.

Ostrosky-Zeichner, L., Casadevall, A., Galgiani, J.N., Odds, F.C., and Rex, J.H. (2010). An insight into the antifungal pipeline: selected new molecules and beyond. Nat. Rev. Drug Discov. *9*, 719–727.

Perrone, G.G., Tan, S.X., and Dawes, I.W. (2008). Reactive oxygen species and yeast apoptosis. Biochim. Biophys. Acta *1783*, 1354–1368.

Phillips, A.J., Sudbery, I., and Ramsdale, M. (2003). Apoptosis induced by environmental stresses and amphotericin B in Candida albicans. Proc. Natl. Acad. Sci. USA *100*, 14327–14332.

Ribeiro, G.F., Côrte-Real, M., and Johansson, B. (2006). Characterization of DNA damage in yeast apoptosis induced by hydrogen peroxide, acetic acid, and hyperosmotic shock. Mol. Biol. Cell *17*, 4584–4591.

Salmon, T.B., Evert, B.A., Song, B., and Doetsch, P.W. (2004). Biological consequences of oxidative stress-induced DNA damage in Saccharomyces cerevisiae. Nucleic Acids Res. *32*, 3712–3723.

Schmitt, M.E., Brown, T.A., and Trumpower, B.L. (1990). A rapid and simple method for preparation of RNA from Saccharomyces cerevisiae. Nucleic Acids Res. *18*, 3091–3092.

Shakoury-Elizeh, M., Protchenko, O., Berger, A., Cox, J., Gable, K., Dunn, T.M., Prinz, W.A., Bard, M., and Philpott, C.C. (2010). Metabolic response to iron deficiency in Saccharomyces cerevisiae. J. Biol. Chem. *285*, 14823–14833.

Soufi, B., Kelstrup, C.D., Stoehr, G., Fröhlich, F., Walther, T.C., and Olsen, J.V. (2009). Global analysis of the yeast osmotic stress response by quantitative proteomics. Mol. Biosyst. *5*, 1337–1346.

Steininger, S., Ahne, F., Winkler, K., Kleinschmidt, A., Eckardt-Schupp, F., and Moertl, S. (2010). A novel function for the Mre11-Rad50-Xrs2 complex in base excision repair. Nucleic Acids Res. *38*, 1853–1865.

Thevelein, J.M., and de Winde, J.H. (1999). Novel sensing mechanisms and targets for the cAMP-protein kinase A pathway in the yeast Saccharomyces cerevisiae. Mol. Microbiol. *33*, 904–918.

Thevissen, K., Ayscough, K.R., Aerts, A.M., Du, W., De Brucker, K., Meert, E.M., Ausma, J., Borgers, M., Cammue, B.P., and François, I.E. (2007). Miconazole induces changes in actin cytoskeleton prior to reactive oxygen species induction in yeast. J. Biol. Chem. *282*, 21592–21597.

Tomas, E., Stanojevic, V., and Habener, J.F. (2011). GLP-1-derived nonapeptide GLP-1(28-36)amide targets to mitochondria and suppresses glucose production and oxidative stress in isolated mouse hepatocytes. Regul. Pept. *167*, 177–184.

Touati, D., Jacques, M., Tardat, B., Bouchard, L., and Despied, S. (1995). Lethal oxidative damage and mutagenesis are generated by iron in delta fur mutants of Escherichia coli: protective role of superoxide dismutase. J. Bacteriol. *177*, 2305–2314.

Walther, T., Novo, M., Rössger, K., Létisse, F., Loret, M.O., Portais, J.C., and François, J.M. (2010). Control of ATP homeostasis during the respiro-fermentative transition in yeast. Mol. Syst. Biol. *6*, 344.

Wickerham, L.J. (1946). A critical evaluation of the nitrogen assimilation tests commonly used in the classification of yeasts. J. Bacteriol. *52*, 293–301.

Winzeler, E.A., Shoemaker, D.D., Astromoff, A., Liang, H., Anderson, K., Andre, B., Bangham, R., Benito, R., Boeke, J.D., Bussey, H., et al. (1999). Functional characterization of the S. cerevisiae genome by gene deletion and parallel analysis. Science *285*, 901–906.

Yan, L., Zhang, J.D., Cao, Y.B., Gao, P.H., and Jiang, Y.Y. (2007). Proteomic analysis reveals a metabolism shift in a laboratory fluconazole-resistant Candida albicans strain. J. Proteome Res. *6*, 2248–2256.

Supplemental Information

Cell PRESS
Open ACCESS

EXTENDED RESULTS

Caspofungin Induces ROS Production and Metabolic Changes Consistent with the Common Mechanism of Antifungal-Induced Cellular Death

The key metabolic changes observed after AF treatment may act as a possible fingerprint to test whether other unrelated AFs may be acting through a similar common mechanism. Caspofungin belongs to a new class of AFs, termed echinocandins, that function by inhibiting cell wall synthesis in *C. albicans* (Denning, 2003). To test if AFs from this class of cidal drugs could induce metabolic changes comparable to the common mechanism of AF-induced cellular death in *C. albicans*, we treated exponentially growing cells with caspofungin and conducted metabolic analyses. We found that the metabolic changes induced by caspofungin were similar to the changes induced by AMB, MCZ and CIC, respectively (Figure S4A–S4C). Specifically, we found an elevation of sugars and a reduction in fermentative byproducts. We also found that caspofungin treatment led to elevated ROS levels in *C. albicans* (Figure S4D). These data indicate that caspofungin acts via a similar common mechanism.

EXTENDED EXPERIMENTAL PROCEDURES

Antifungal Drugs

AF drugs were resuspended at 250 times the working concentration in DMSO (CIC was solubilized in ethanol) and frozen at 80°C in one-time-use aliquots. DMSO was added to cells at 0.4% as the no-treatment control. To account for observed potency differences between different lots of AF drugs, each set of experiments was performed using frozen stocks from the same lot. Each AF drug was titrated against *S. cerevisiae* and *C. albicans* in order to identify the minimal fungicidal concentration. This drug concentration was used for the phenotypic assays in order to achieve maximal sensitivity for resistant mutants.

Fungicidal Killing and Fluorescent Dye Assays

Overnight yeast cultures were diluted into the indicated media and grown to an OD600 of 0.2, at which point the AFs were added. Colony forming units (CFU) were measured by plating six serial dilutions onto YPD agar plates. Cells treated with MCZ were washed before serial dilution to stop growth inhibition associated with high concentrations of MCZ. CFU were counted after 48 hours of incubation on agar plates. When indicated, thiourea (Fluka) was added 30 min prior to the addition of AFs. HPF (10 μM) (Invitrogen) and *MitoTracker* (1 μM) (Invitrogen) dyes were added to PBS-washed cells at the indicated time points and incubated for 30 min prior to flow cytometry measurements, which were taken on the FACSCalibur (Becton Dickinson). All experiments described in this section were conducted in 0.5 ml of SDC in 24-well plates incubated at 900 rpm and 37°C for *C. albicans* and 30°C and 300 rpm for *S. cerevisiae*. TUNEL assays were conducted as previously described (Ribeiro et al., 2006) and are described in detail in the TUNEL section of the Extended Experimental Procedures.

High-Throughput 96-Well Screen

To identify genes critical to AF action, we chose to test the AF sensitivity of single-gene knockouts identified through our common transcriptional analysis. In the first pass-through, we identified 56 testable genes. This set was later expanded to include targets identified through phenotypic analysis and metabolomic profiling, for a total of 84 target genes (Table S1). We tested the initial 56 targets using a rapid high-throughput 96-well assay with AMB and MCZ to identify single-gene knockouts with elevated resistance to AFs (Table S1). Knockouts that were more resistant to at least one of the AFs were tested individually using the 24-well colony forming (CF) assay. Target genes selected after the initial 56 strains were assayed individually using the 24-well CF assay.

The first 56 *S. cerevisiae* strains were acquired from the deletion library and stored in 96-well plates in replicates of three. To start the assay, the plates were defrosted and 10 μl of stored cells were inoculated into 100 μl of fresh synthetic dextrose complete (SDC) media for 16 hr. These overnight cultures were diluted into a fresh 96-well plate with 100 μl of SDC to achieve an OD600 of approximately 0.2. Colony forming units (CFU) in each well were measured at the start of the assay and after 8 hr of incubation. The AF susceptibility of each strain was compared to that of wild-type. Strains with significant susceptibility differences from wild-type were assayed in 0.5 ml of SDC media using the 24-well plate CF assay described above.

Metabolomic Profiling

C. albicans cells were incubated in 100 ml of SDC in 250 ml flasks at 37°C and 300 rpm. Cells were exposed to AFs at an OD600 of 0.2, and cellular pellets from 100 ml of media were collected after 1.5 hr of treatment. Cells were lysed and assayed by Metabolon Inc. (Durham, USA) as previously described (Evans et al., 2009; Shakoury-Elizeh et al., 2010).

ATP and AMP Measurements

To quantitate the cellular AMP/ATP ratio, *C. albicans* cells were incubated in 25 ml of SDC in 250 ml flasks at 37°C and 300 rpm. AF drugs were added at an OD600 of 0.2, and 2 ml of cells were collected every 10 min for the first 90 min of incubation. Cells were lysed and nucleotides were extracted using boiling buffered methanol as previously described (Walther et al., 2010). Lysates were

desiccated and resuspended in 60 ml of water prior to HPLC analysis. Nucleotides were separated isocratically in 100 mM sodium phosphate pH 6.5 on a ZORBAX SIL SAX 70Å 5um, 4.6 × 150mm column (Agilent, Santa Clara CA).

S. cerevisiae Microarrays

Yeast cells were incubated in 25 ml of SDC and grown in 250ml flasks at 30°C and 300 rpm. AFs were added at an OD600 of 0.2.

Yeast cells were incubated in 25 ml of SDC and grown in 250 ml flasks at 30°C and 300 rpm. Antifungals were added at an OD600 of 0.2. The rate of yeast killing by MCZ and CIC, respectively, was reduced by the transition from the 0.5 ml culture to 25 ml cultures. Rather than increasing drug concentration to match 0.5 ml killing levels, CIC and MCZ samples were collected after extending incubation times to achieve killing levels comparable to the 0.5 ml experiments. RNA from untreated cells was collected at 0, 0.5, 1 and 2 hr after treatment. RNA from AMB-treated cells was collected at 0.5, 1 and 2 hr after treatment. RNA from MCZ-treated cells was collected at 2, 5 and 8 hr after treatment. Cellular RNA was isolated and processed as previously described (Schmitt et al., 1990).

The effect of AF treatment on *S. cerevisiae* global gene expression was assayed using Affymetrix yeast microarrays (Affymetrix GeneChip Yeast Genome 2.0 array). The collected microarray data were added to a compendium of publicly available microarrays (obtained from the Gene Expression Omnibus) for a total of 536 chips. The set of expression profiles was normalized as a batch with RMA Express (Bolstad et al., 2003). The SD of the expression of each gene was calculated across the entire compendium of expression profiles, allowing us to calculate a *z*-scale difference between a treatment and a control condition (no-treatment) using the formula:

$$\Delta z_{exp} = \frac{X_{exp} - X_{ctr}}{\sigma}$$

This allowed us to determine gene expression changes in units of standard deviation, which is a form of the *z*-test. For each of the time points in each treatment, the *z*-score difference was converted into *p-value*s and the sets of up- and downregulated genes ($p < 0.05$) were identified. The set of differentially expressed genes was merged across all time points, resulting in a global set of differentially expressed genes in AF-treated cells as compared to untreated cells. A common set of genes differentially expressed in response to all three antifungal drug treatments was determined by the intersection of the three distinct gene sets (Figures 1D and 1E).

TUNEL Assay

DNA strand breaks were fluorescently labeled with TUNEL reagent from the "In Situ Cell Death Detection Kit," Roche (Mannheim, Germany). After 2 hr of treatment 5 ml of OD 0.2 cells were fixed with 3.7% formaldehyde for 30 min at room temperature, and then washed with digestion buffer consisting of 10 mM Mes pH 6.5 and 1 M sorbitol. Cell were digested for 45 min at 30°C with 2 U of Yeast Lytic Enzyme, MP Biomedicals, (Irvine, CA) in 50 μl of digestion buffer. Cells were then washed in PBS with 1 M sorbitol and resuspended in permeabilization solution consisting of 0.1% Triton X-100 and 0.1% sodium citrate and 1 M sorbitol for 10 min at room temperature. Cell were again washed in PBS with 1 M sorbitol and labeled for 60 min with 10 μl of TUNEL reaction mixture. Cells were then again washed in PBS with 1 M sorbitol and resuspended in sheath fluid. Mean relative florescence was measured by flow cytometry on the FACSCalibur (Becton Dickinson).

SUPPLEMENTAL REFERENCES

Bolstad, B.M., Irizarry, R.A., Astrand, M., and Speed, T.P. (2003). A comparison of normalization methods for high density oligonucleotide array data based on variance and bias. Bioinformatics *19*, 185–193.

Denning, D.W. (2003). Echinocandin antifungal drugs. Lancet *362*, 1142–1151.

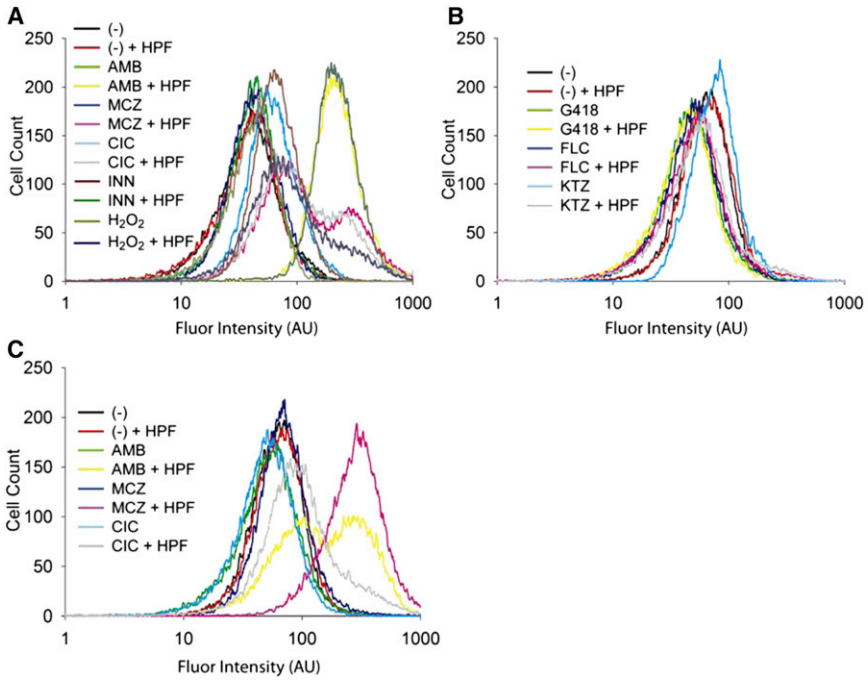

Figure S1. Fungicide-Dependent ROS Production, Related to Figure 1

(A–C) Generation of hydroxyl radicals measured by a change in 3′-(p-hydroxyphenyl) fluorescein (HPF) fluorescence after 1.5 hr of drug exposure. (A and B) *S. cerevisiae* exposed to cidal and static drugs, respectively. (C) *C. albicans* exposed to cidal drugs. Chromatographs of treated cells without HPF incubation are included to demonstrate the HPF-dependent change in fluorescence for each treatment. Drug concentrations used: AMB 1 μg/ml, MCZ 50 μg/ml, CIC 75 μg/ml, H_2O_2 1 mM, geneticin (G418) 100 μg/ml, fluconazol (FLC) 50 μg/ml, 5-flucytosine (5-FC) 15 μg/ml, and ketoconazole (KTZ) 50μg/ml.

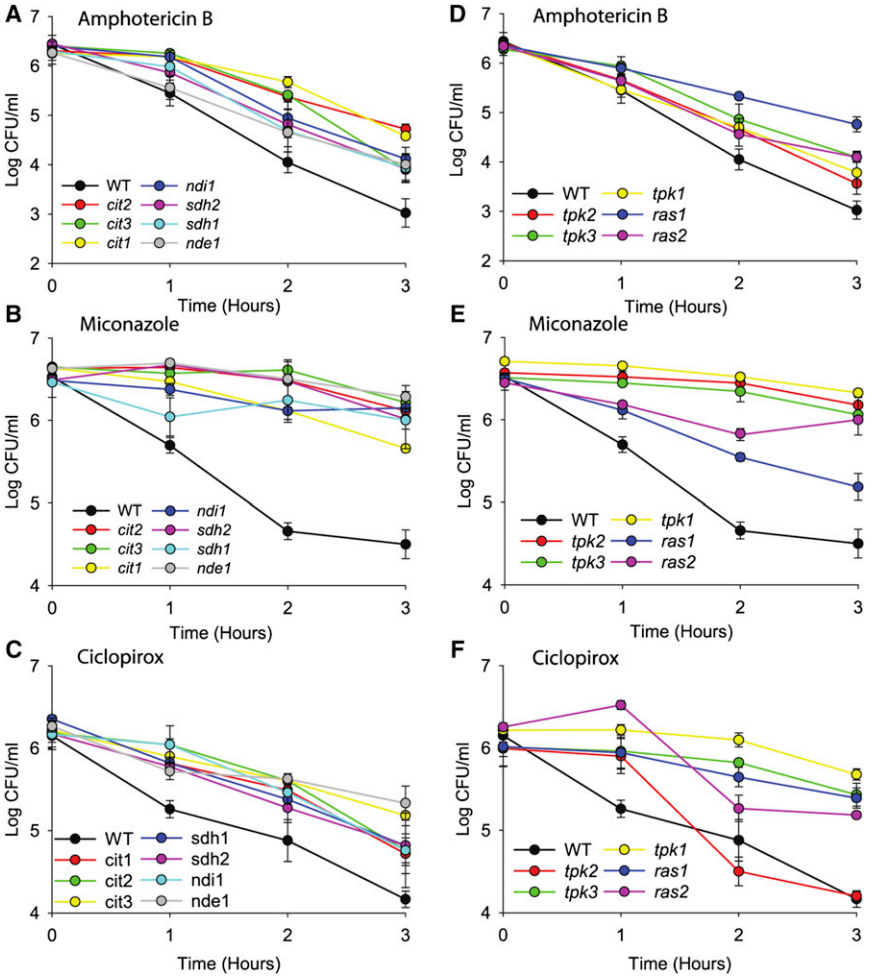

Figure S2. TCA-Dependent Respiration and the Ras/PKA Pathway Play a Critical Role in Antifungal-Induced Cell Death, Related to Figure 2

(A–F) Log of CFU/ml remaining after drug exposure. Drug concentrations used: AMB 1 μg/ml, MCZ 50 μg/ml, and CIC 75 μg/ml. The reported error is standard deviation (s.d.) with $n \geq 3$.

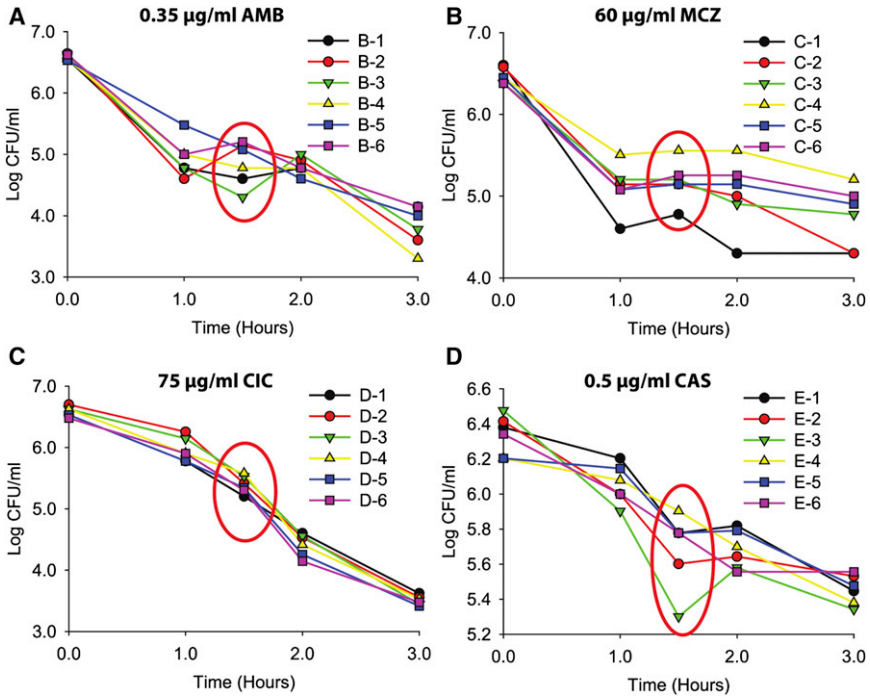

Figure S3. Kill Curves of Metabolically Profiled *C. albicans* Cultures, Related to Figure 3

(A–D) Log of CFU/ml remaining after exposure of wild-type *C. albicans* to the indicated drug concentrations. Cells were collected at the time point indicated by the red oval and sent for metabolomic profiling. The letter and number combinations refer to specific samples that were metabolically profiled and are consistent with the labels in Data Set S1.

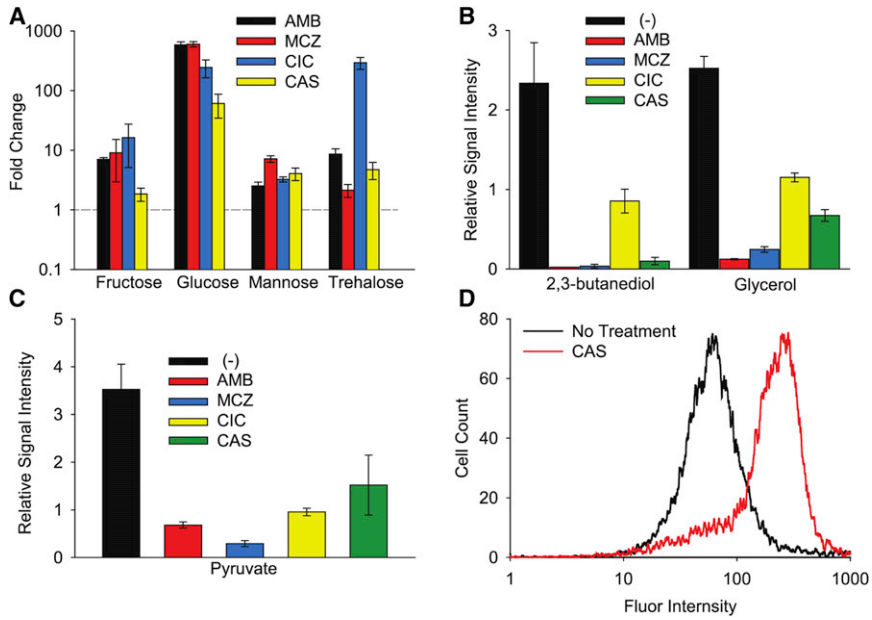

Figure S4. Caspofungin-Induced Metabolic Changes Match the Changes Predicted by the Common Mechanism, Related to Figure 3

(A) Fold change in metabolite levels compared to the no-treatment control.

(B and C) Relative signal intensity of select metabolites identified through metabolomic profiling of *C. albicans* exposed to antifungal drugs for 1.5 hr. Drug concentrations used: AMB 1 μg/ml, MCZ 50 μg/ml, CIC 75 μg/ml and caspofungin (CAS) 0.5 μg/ml. The reported error is standard error mean with n = 6.

(D) Generation of hydroxyl radicals measured by a change in 3′-(p-hydroxyphenyl) fluorescein (HPF) fluorescence after 1.5 hr of exposure to CAS at 0.5 μg/ml. Caspofungin acetate was provided by Merck Research Laboratories (Rahway, NJ).